Crystallization Studies of $Al_{85}Y_{10}Fe_{5-x}Ni_x$ (x = 0, 2.5, 5) Alloys

Musa Gögebakan

(Submitted 30 April 2003)

The crystallization behavior of melt-spun $A_{85}Y_{10}Fe_{5-x}N_x$ (x = 0, 2.5, 5) amorphous alloys has been investigated by a combination of differential scanning calorimetry (DSC) and x-ray diffractometry (XRD). XRD traces of these alloys consisted of a single broad peak corresponding to fully amorphous structure. Continuous DSC results showed that, the first crystallization peak temperature of $Al_{85}Y_{10}Fe_5$ amorphous alloy was about 60 K higher than that of $Al_{85}Y_{10}Ni_5$. The activation energies for the first crystallization peak increased from 210 kJ/mol for $Al_{85}Y_{10}Ni_5$ to 280 for $Al_{85}Y_{10}Fe_5$. These results indicate that 5 at.% substitutions Ni by Fe increases the stability of the amorphous phase.

Keywords activation energy, AlYFeNi alloy, crystallization

1. Introduction

Rapid solidification is now widely used as a technique to prepare materials in the amorphous states[1,2] or other nonequilibrium states.[3,4] Numerous rapidly solidified Al-based amorphous alloys with high strength and good ductility have been reported during the past three decades. These Al-based amorphous alloys exhibit high tensile strength above 1000 MPa.[5] It has recently been reported that the homogeneous dispersion of nanoscale Al particles in an amorphous matrix of Al-Ni-RE (RE is rare earth metals)[6] and Al-Ni-RE-M (M = Fe, Co, or Mn)[7,8] caused an increased in the tensile fracture strength of about 1.5 times compared with the corresponding amorphous single-phase alloys. The significant increase in the strength of mixed phases alloys has been attributed to the presence of the defect-free Al particles, which act as effective barriers to shear deformation of the amorphous matrix.[6] Therefore, Al-based amorphous alloys have found practical application as high strengths materials with lightweight and high corrosion resistance. The purpose of the current study was to investigate the crystallization behavior of amorphous $Al_{85}Y_{10}Fe_{5-x}Ni_x$ (x = 0, 2.5, 5) alloy using a combination of differential scanning calorimetry (DSC) and x-ray diffractometry (XRD).

2. Experimental Work

The $Al_{85}Y_{10}Fe_5$, $Al_{85}Y_{10}Fe_{2.5}Ni_{2.5}$, and $Al_{85}Y_{10}Ni_5$ master alloys were prepared by induction melting of high purity elements under argon atmosphere. The melt-spinning experiments were carried out on a single Cu roller at a circumferential wheel speed of 40 m/s. Melt-spun ribbons were typically several meters long, 3 mm wide, and 30 μm thick. The amorphous nature of the melt-spun ribbons was characterized by XRD using a Philips PW 1729 x-ray diffractometer (Analytical B.V., Almelo, The Netherlands) with filtered CuKα. The crystallization behavior of the amorphous melt-spun ribbons was studied by DSC using a combination of continuous heating from 350-750 K at a constant heating rate of 20 K/min inside a TA2200 thermal analyzer with TA2010 DSC cell. The composition of the melt-spun ribbons was determined using a CAMECA SU30 electron microscope (Kinetica, Inc, Franklin, Ohio) equipped with wavelength dispersive x-ray analysis (WDS) facilities.

Musa Gögebakan, Department of Physics, Faculty of Art and Science, Kahramanmaras Sutcu Imam University, 46100 Kahramanmaras, Turkey. Contact e-mail: gogebakan24@hotmail.com.

3. Results and Discussion

Table 1 lists the composition of the melt-spun $A_{85}Y_{10}Fe_{5-x}N_x$ (x = 0, 2.5, 5) alloys determined using WDS.

Figure 1 shows typical XRD traces of the as-melt-spun $Al_{85}Y_{10}Fe_5$, $Al_{85}Y_{10}Fe_{2.5}Ni_{2.5}$ and $Al_{85}Y_{10}Ni_5$ alloys produced under nominally the same processing conditions at a circumferential wheel speed of 40 m/s. All three traces show a single broad peak (2θ~38°), indicating a fully amorphous structure. It has been reported that rare earth (Y) plays an important role in the glass forming ability of this alloy systems.[1,9] Figure 2 shows continuous heating DSC traces obtained from the as-melt-spun $Al_{85}Y_{10}Fe_5$, $Al_{85}Y_{10}Fe_{2.5}Ni_{2.5}$, and $Al_{85}Y_{10}Ni_5$ alloys prepared under nominally the same processing conditions. The data for different compositions are shifted vertically to avoid overlap. The continuous heating DSC traces consisted of two exothermic peaks for $Al_{85}Y_{10}Fe_5$ alloy, and three exothermic peaks for $Al_{85}Y_{10}Fe_{2.5}Ni_{2.5}$ and $Al_{85}Y_{10}Ni_5$ alloys. $Al_{85}Y_{10}Fe_5$ exhibits a first exothermic peak at 588 K and second exothermic peak with peak temperature of 711 K. $Al_{85}Y_{10}Fe_{2.5}Ni_{2.5}$ exhibits a first exothermic peak at 586 K followed by two exothermic peaks at 630 and 682 K, respectively. $Al_{85}Y_{10}Ni_5$ exhibits a relatively small broad exothermic peak with a peak temperature of 525 K, and second and third exothermic peaks with peak temperatures of 598 and 663 K, respectively. The first crystallization peak temperature increased from 525 K for $Al_{85}Y_{10}Ni_5$ to 588 K for $Al_{85}Y_{10}Fe_5$. This indicates that 5 at.% substitutions Ni by Fe increase the

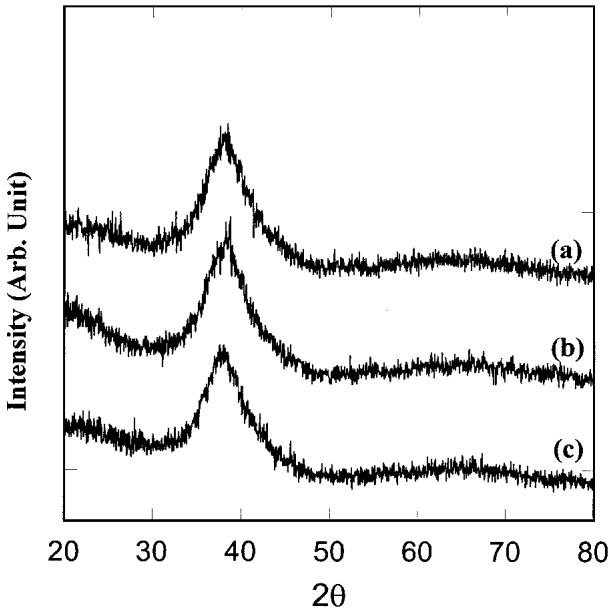

Fig. 1 XRD spectra from the as-melt-spun: **(a)** $Al_{85}Y_{10}Fe_5$, **(b)** $Al_{85}Y_{10}Fe_{2.5}Ni_{2.5}$, and **(c)** $Al_{85}Y_{10}Ni_5$ alloys

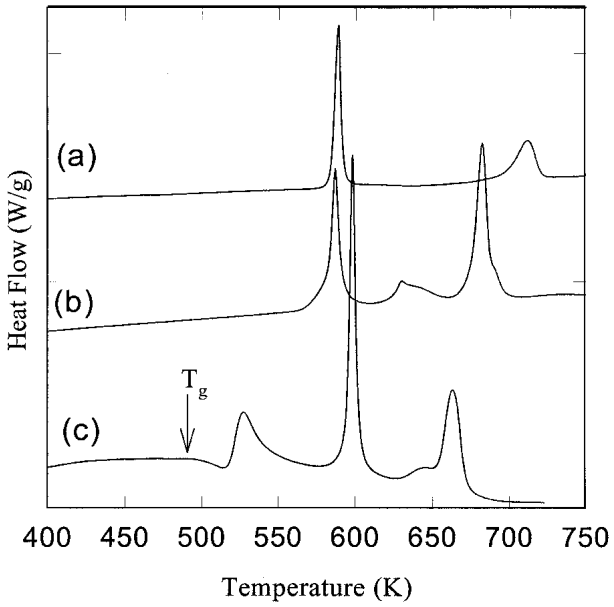

Fig. 2 DSC traces from the as-melt-spun: **(a)** $Al_{85}Y_{10}Fe_5$, **(b)** $Al_{85}Y_{10}Fe_{2.5}Ni_{2.5}$, and **(c)** $Al_{85}Y_{10}Ni_5$ alloys

Table 1 List of Measured Composition of the Melt-Spun $A_{85}Y_{10}Fe_{5-x}N_x$ (x = 0, 2.5, 5) Alloys

Nominal Composition, at.%	Measured Composition, at.%
$Al_{85}Y_{10}Fe_5$	$Al_{86}Y_{9.4}Fe_{4.6}$
$Al_{85}Y_{10}Fe_{2.5}Ni_{2.5}$	$Al_{85.5}Y_{9.2}Fe_{2.4}Ni_{2.9}$
$Al_{85}Y_{10}Ni_5$	$Al_{85.8}Y_{9.6}Ni_{4.6}$

Table 2 Activation Energies E_a, kJ/mol, for Crystallization in $Al_{85}Y_{10}Fe_5$, $Al_{85}Y_{10}Fe_{2.5}Ni_{2.5}$, and $Al_{85}Y_{10}Ni_5$ Alloys

Alloys	E_1	E_2	E_3
$Al_{85}Y_{10}Fe_5$	280	235	
$Al_{85}Y_{10}Fe_{2.5}Ni_{2.5}$	265	220	200
$Al_{85}Y_{10}Ni_5$	210	275	185

stability of the amorphous phase. On the other hand continuous DSC traces showed that glass transition temperature (T_g) and subsequent supercooled liquid region was only observed for $Al_{85}Y_{10}Ni_5$ alloy as an endothermic effect just before the first crystallization peak, marked by arrows in Fig. 2(c). The glass transition behavior is an important characteristic of Al-based amorphous alloy system,[10] because the glass transition reflects atomic transport and viscosity properties that are dominant factors in the glass forming-ability of alloys and in the structural relaxation and thermal stability of the amorphous structure. The temperature interval of the supercooled liquid region defined by the difference between glass transition temperature (T_g) and the first crystallization temperature (T_x), ΔT_x ($= T_x - T_g$) is found to be around 25 K. The atomic diffusivity in this temperature region above T_g is expected to be large. Internal equilibrium is achieved within the amorphous structure because of very short relaxation times but nevertheless crystallization is still inhibited. The existence of a wide supercooled liquid region in Al-based amorphous alloys is an important technological finding. The supercooled liquid in the ΔT_x region has a low viscosity and materials can flow deform easily.[10] This allows bulk amorphous materials to be produced either by warm consolidation or pressing of amorphous powders. A large ΔT_x value indicates that the supercooled liquid has a high thermal stability against crystallization. In other words, it is expected that alloys with a large ΔT_x value should also have a large glass-forming ability.

Kinetic analysis for crystallization of these alloys was performed by calculating the activation energy using the Kissinger method,[11] and results are presented in Table 2. The activation energies for the first crystallization peak increased from 210 kJ/mol for $Al_{85}Y_{10}Ni_5$ to 280 kJ/mol for $Al_{85}Y_{10}Fe_5$. This result also indicates that 5 at% substitutions Ni by Fe increase the stability of the amorphous phase. However, the general relationship between alloy stability and the activation energy associated with the first crystallization reaction is clearly seen by comparing the first crystallization peak temperature and the first crystallization peak activation energy. Both of these quantities are largest for the $Al_{85}Y_{10}Fe_5$ alloy. This suggests a relationship between the decrease in atomic mobility, as shown by an increase in the first peak activation energy during crystallization, and the increase in the thermal stability of the alloy.

4. Conclusions

In this study the crystallization behavior of $Al_{85}Y_{10}Fe_5$, $Al_{85}Y_{10}Fe_{2.5}Ni_{2.5}$, and $Al_{85}Y_{10}Ni_5$ amorphous alloys were examined. The continuous heating DSC traces consisted of two exothermic peaks for $Al_{85}Y_{10}Fe_5$ alloy, and three exothermic peaks for $Al_{85}Y_{10}Fe_{2.5}Ni_{2.5}$ and $Al_{85}Y_{10}Ni_5$ alloys. The first

crystallization peak temperature increased from 525 K for $Al_{85}Y_{10}Ni_5$ to 588 K for $Al_{85}Y_{10}Fe_5$. Activation energies of these amorphous alloys were determined by using Kissinger method. The activation energies for the first crystallization peak increased from 210 kJ/mol for $Al_{85}Y_{10}Ni_5$ to 280 kJ/mol for $Al_{85}Y_{10}Fe_5$. This indicates that 5 at.% substitutions Ni by Fe increase the stability of the amorphous phase.

Acknowledgment

The author thanks Kahramanmaras Sutcu Imam University for financial support of the research program.

References

1. R. Sabet-Sharghi, Z. Altounian, and W.B. Muir: "Formation, Structure and Crystallization of Al-Rich Metallic Glasses," *J. Appl. Phys.,* 1994, *75*(9), pp. 4438-41.
2. A.K. Gangopadhyay and K.F. Kelton: "Effect of Rare-Earth Atomic Radius on the Devitrification of $Al_{88}RE_8Ni_4$ Amorphous Alloys," *Phil. Mag. A*, 2000, *80*(5), pp. 1193-206.
3. W. Lui and U. Köster: "Decomposition of the Icosahedral Phase in Al-Cu-Fe Alloys," *Mater. Sci. Eng. A*, 1991, *133,* pp. 388-92.
4. S.J. Hong, P.J. Warren, and B.S. Chun: "Nanocrystallization Behaviour of Al-Y-Ni With Cu Additions," *Mater. Sci. Eng. A*, 2001, *304-306*, pp. 362-66.
5. A. Inoue, K. Ohtera, A.P. Tsai, and T. Masumoto: "Aluminum-Based Amorphous Alloys With Tensile Strength Above 980 MPa (100 kg/mm^2)," *Jap. J. Appl. Phys*., 1988, *27,* pp. L479-82.
6. Y.H. Kim, A. Inoue, and T. Masumoto: "Increase in Mechanical Strength of Al-Y-Ni Amorphous Alloys by Dispersion of Nanoscale fcc-Al Particles," *Mater. Trans. JIM*., 1991, *32,* pp. 331-38.
7. Y.H. Kim, A. Inoue, and T. Masumoto: "Ultrahigh Tensile Strengths of $Al_{88}Y_2Ni_9M_1$ (M = Mn or Fe) Amorphous Alloys Containing Finely Dispersed fcc-Al Particles," *Mater. Trans. JIM.*, 1990, *31,* pp. 747-49.
8. Y.H. Kim, A. Inoue, and T. Masumoto: "Ultrahigh Mechanical Strengths of $Al_{88}Y_2Ni_{10-x}M_x$ M = Mn, Fe, Co) Amorphous Alloys Containing Nanoscale fcc-Al Particles," *Mater. Trans. JIM.,* 1991, *32,* pp. 599-608.
9. M. Gögebakan: "Amorphous and Nanocrystalline Al-Based Alloys," Ph.D. Thesis, University of Oxford, Oxford, UK, 1998.
10. A. Inoue, N. Matsumoto, and T. Masumoto: "Al-Y-Ni-Co Amorphous Alloys With High Mechanical Strengths, Wide Supercooled Liquid Region and Large Glass-Forming Capacity," *Mater. Trans. JIM*., 1990, *31*, pp. 493-500.
11. H.E. Kissinger: "Reaction Kinetics in Differential Thermal Analysis," *Anal. Chem.*, 1957, *29,* pp. 1702-06.